Development of the sequential combustion system for the GT24/GT26 gas turbine family

The 60-Hz, 165-MW GT24 and the 50-Hz, 265-MW GT26 are the first two members of ABB's new gas turbine family based on sequential combustion. These turbines offer higher output plus an efficiency advantage of up to 4 % over today's machines. Whereas the first combustor in the sequential combustion system employs proven EV combustor technology, the lean premixed, self-igniting second combustor is the result of an extensive R&D programme that included wind tunnel and water channel experiments, computational fluid dynamics (CFD) calculations and combustion tests at atmospheric and high pressure. An innovative cooling technology was also developed to satisfy the special needs of the self-igniting premix combustor. The test programme further showed that the sequential combustion system has the potential to lower NO_x emissions to single-digit levels.

The GT24/GT26 gas turbine family 1 uses proven turbine technology and applies it in a unique manner to solve a problem that has challenged the power generation industry since the inception of advanced technology: the uncoupling of efficiency and emissions.

In standard gas turbine designs, the higher turbine inlet temperature required for increased efficiency results in higher emission levels and increased material and life cycle costs.

This problem is overcome with the sequential combustion cycle. Such a cycle forms the basis of ABB's advanced GT24 (60 Hz) and GT26 (50 Hz) gas turbines, which combine compactness with high specific power, high efficiency, high reliability and low emissions.

Dr. Franz Joos
Philipp Brunner
Dr. Burkhard Schulte-Werning
Dr. Khawar Syed
ABB Power Generation

Dr. Adnan Eroglu
ABB Corporate Research

GT24/GT26 performance data

Rated at 165 MW, the GT24 delivers 50 % more output than a conventional GT11N2 with essentially the same footprint of 10 × 5 meters. The higher output is the result of increases in the cycle pressure ratio and the sequential combustion cycle. Additionally, the exhaust temperature of the GT24/GT26 is 610°C (1130 °F), which is ideal for combined cycle (gas and steam turbine plant) operation (*Table 1*).

Scaled up from the GT24, the GT26 is for the 50-Hz market, with an output of 265 MW and efficiencies of 38.2 % in simple cycle and 58.5 % in combined cycle mode.

The power density of this gas turbine family is approximately 20 % higher than for other units in this class. This allows a more compact design, shorter blade lengths, lower tip speeds and therefore lower stresses, leading to higher reliability.

Sequential combustion system

From the outside, the straight through-flow design of the GT24/GT26 gas turbines looks very similar to that of a conventional gas turbine, with a cold-end generator drive, the air intake system perpendicular to the shaft, axial turbine exhaust and all casings and vane carriers split horizontally. The main developments that led to the advanced and compact GT24/26 turbine design have already proved their reliability in numerous power plants.

The advanced technology behind the GT24/GT26 is the sequential com-

This article is based on a paper of the same title, presented at the ASME Turbo Expo '96 in Birmingham, UK. It was named 'Best Technical Paper' by the Electric Utilities & Cogeneration Committee at Turbo Expo '97 and honoured with the 1996 ASME Award for its outstanding contribution to the literature of gas turbines and power plants at ASME TURBO EXPO '98.

bustion system 2. With a pressure ratio of 30:1, the compressor delivers nearly double the pressure ratio of a conventional compressor, although in terms of applied technology it remains well within the experience envelope [14]. The compressed air is heated in a first combustion chamber (EV combustor). After the addition of about 60 % of the fuel (at full load), the combustion gas expands through the first turbine stage. This one-stage, high-pressure (HP) turbine lowers the pressure from 30 to approximately 15 bar.

The remaining fuel is added in a second combustion chamber (SEV combustor), where the gas is again heated to the maximum turbine inlet temperature. Final expansion in the 4-stage, low-pressure (LP) turbine follows. 3 shows the thermodynamic cycle of the sequential combustion process, while 4 compares the cycle of the sequential combustion process with a conventional cycle. It is seen that for the same power output, a lower turbine inlet temperature is needed with the sequential combustion cycle.

Sequential combustion is not new in the history of power generation. ABB delivered already during the 1950s and 1960s 24 plants with various combinations of intercooling in the compressor and two-stage combustion in the turbine. Nine of these plants are still in operation today. ABB therefore has decades of experience with sequential combustion systems [7].

Design features of the GT24/GT26 EV combustor

The first combustor is an annular combustion chamber equipped with 30 proven dry low-NO_x EV burners. The EV burner (EV stands for 'Environmental') [16] adds the benefit of low NO_x combustion without water or steam injection. First commercially tested in 1990 at the Midland Cogeneration Venture, Michigan (USA), the fleet using the EV burner has meanwhile run up more than 800,000 hours of reliable operation.

The compact annular combustion chamber design is another key component of the sequential combustion system. It is already proven in the GT10 (25-MW) and in the GT13E2 (165-MW) gas turbines [1,17], the latter having been successfully commissioned in Japan in 1993. Launched in 1991, 53 units of the GT13E2 have been ordered to date, with 48 units already in operation.

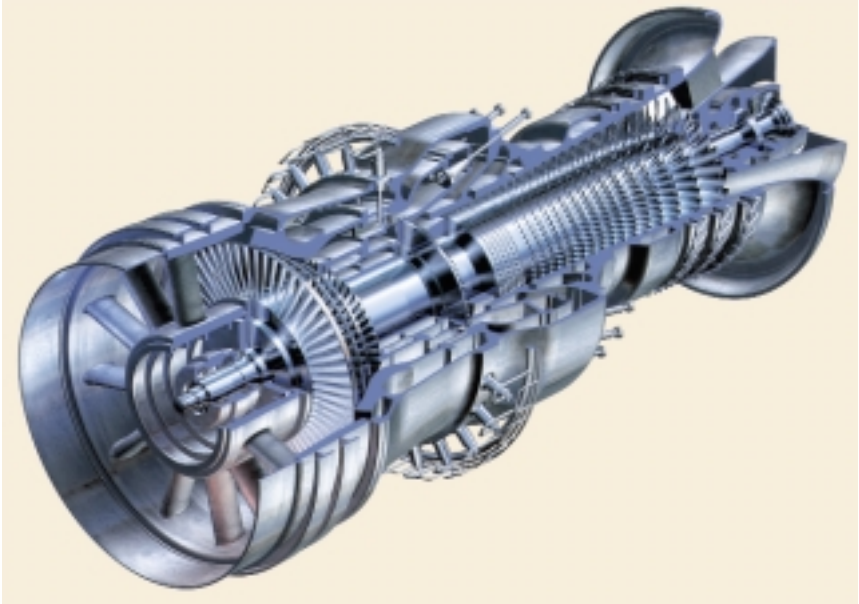

Cutaway drawing of the advanced ABB GT24/GT26 gas turbine 1

Table 1:
Technical data of the GT24 and GT26 gas turbines (simple cycle, methane)

		GT24	*GT26*
Load output*	MW	165	265
Efficiency (LHV)*	%	37.9	38.2
Heat rate (LHV)*	Btu/kWh	9,000	8,930
Compressor ratio	–	30	30
Exhaust mass flow	kg/s	378	545
Exhaust temperature	°C	610	610
Shaft speed	rpm	3,600	3,000
NO_x emissions	vppm	< 25	< 25
No of stages			
compressor	–	22	22
turbine	–	5	5
No and type of annular combustors	–	1 EV	1 EV
	–	1 SEV	1 SEV
No of burners EV/SEV	–	30/24	30/24

* = at generator terminals

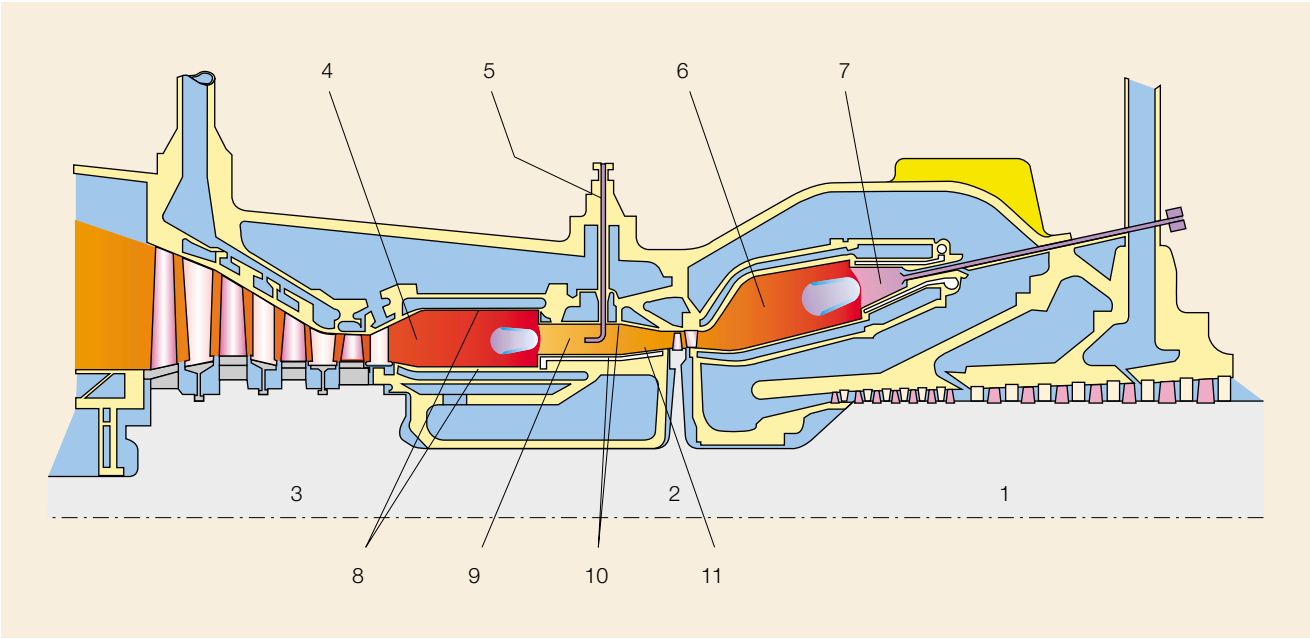

Section through the sequential combustion system in the GT24/GT26 gas turbine **2**

1 *Compressor*
2 *High-pressure turbine*
3 *Low-pressure turbine*
4 *SEV combustor*
5 *Fuel injector*
6 *EV combustor*
7 *EV burner*
8 *Convective liner cooling*
9 *Mixing zone*
10 *Vortex generators*
11 *Effusion-cooled SEV burner*

This very compact combustion chamber has a carrier structure with segmented liners which are cooled by convection. There are no cooling films on the hot side of the walls. Virtually all the incoming compressor air is led to the EV burners, where a lean premix combustion process ensures extremely low NO_x emissions. The EV burners employ the 'vortex breakdown' principle; neither mechanical flame holders nor cross-firing tubes are therefore necessary. All EV burners operate throughout the full load range. The temperature profile of the departing hot gas is very even in the circumferential direction (due to the annular design) as well as in the radial direction (primarily due to the premixing of all air with the fuel and the absence of film cooling of the inner and outer liners of the combustor). This important feature enhances reliability and efficiency in the first turbine stage and increases the lifetime of the hot-gas components.

The SEV combustor – basic considerations

Experimental findings show that for many fuels the weak extinction limit corresponds to an equivalence ratio Φ of around 0.5 in atmospheric conditions and is relatively independent of the pressure. In contrast, the flammability range is considerably widened by increasing the inlet temperature **5**. This widening is generally ascribed to the enhanced flame temperature, which strengthens the diffusion ignition sources in the flame propagation process [5].

At considerably higher temperatures a region is found where self-ignition of the fuel occurs **5** and no external ignition source for flame propagation is required.

Spontaneous ignition delay is defined as the time interval between the creation of a combustible mixture, achieved by injecting fuel into air at high temperatures, and the onset of a flame. In view of their practical importance, measurements of spontaneous ignition delay have been conducted for many fuels over wide ranges of ambient conditions [18, 19]. **6** compares the ignition delay time of methane with that of a typical natural gas and oil no 2.

In a conventional lean premix combustor (eg the EV combustion chamber) spontaneous ignition must be avoided, since it could lead to overheating of combustor components and to unacceptably high pollutant emissions. A reheat combustion system, such as the SEV (Sequential EV) combustion chamber, can be designed to use the self-ignition effect for a simple and rugged construction. In order to achieve reliable spontaneous ignition with natural gas and to widen the stability range, combustor inlet temperatures higher than 1000 °C over the whole operating range were selected for the GT24/GT26 SEV combustor.

Successful operation of the SEV combustor requires that, in addition to ensur-

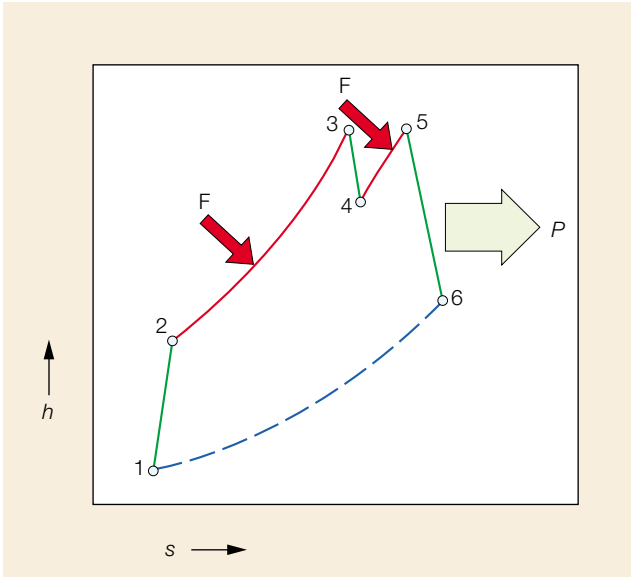

Thermodynamic cycle of the sequential combustion system 3

h Enthalpy
s Entropy
F Fuel input
P Power to generator

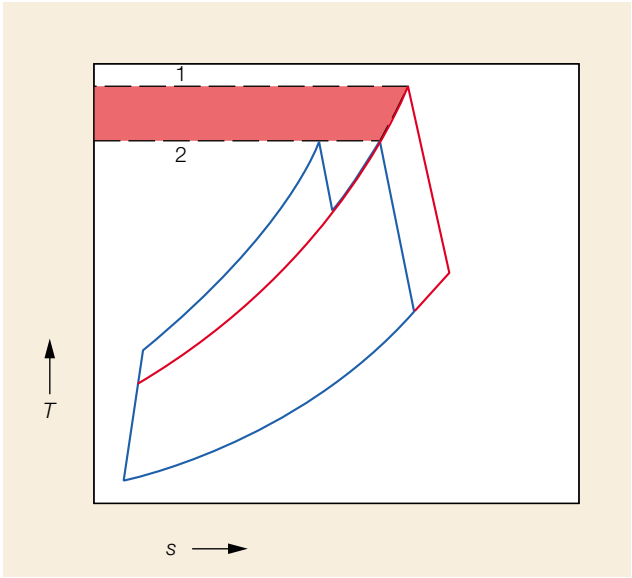

Comparison of the thermodynamic cycle of a sequential combustion concept with that of a conventional concept 4

T Temperature *s* Entropy

1 Standard GT: high turbine inlet temperature
2 Sequential combustion

ing self-ignition, emissions are kept low. For low NO_x emissions the fuel and the hot HP turbine exit gas must be mixed well prior to ignition. If this is not the case burning will occur in fuel-enriched regions, where high flame temperatures result in high NO_x generation rates. An optimum relationship between the ignition delay and degree of premixing is therefore desirable, the former having to be kept short in order to ensure self-ignition and limit the size of the combustor. Furthermore, this optimum should be maintained over a wide range of fuel flow rates, which change with the combustor

Flammability limits with self-ignition (p = 15 bar) 5

T Inlet temperature
CH_4 Methane

1 Self-ignition after 1 ms

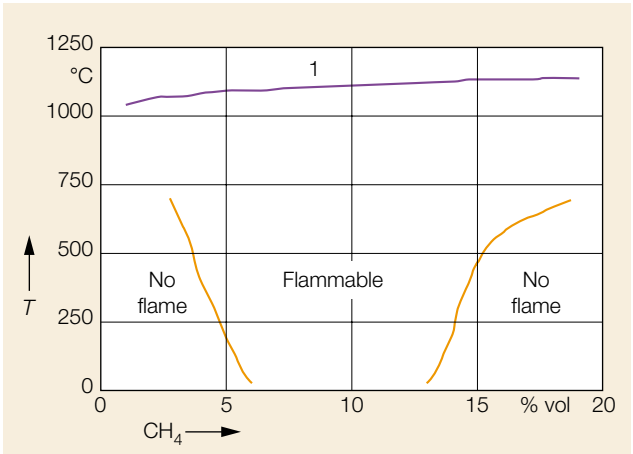

Ignition delay time of methane, natural gas and no 2 oil (pressure = 15 bar, equivalence ratio = 1.0 Φ [18, 19]) 6

τ Ignition delay
T Temperature of mixture

Blue *Methane*
Green *Natural gas*
Red *No 2 oil*

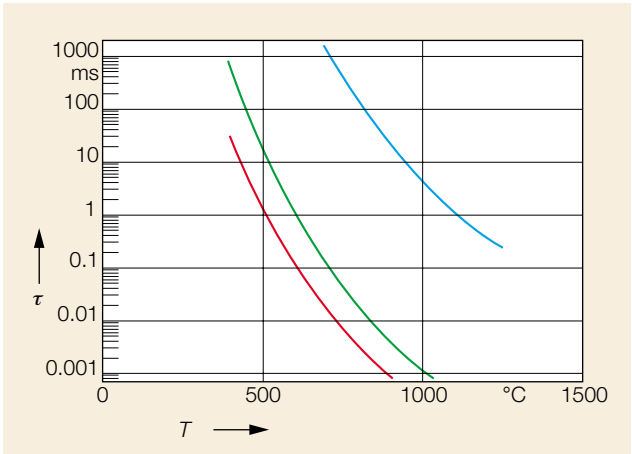

load and fuel compositions, eg as a result of different blends of natural gas.

Fuel injection

In the SEV combustor of the GT24/GT26, the above optimum is reached through the use of carrier air, ie air that is bled from the compressor and injected into the SEV burner together with the fuel. The carrier air works both as a premixing enhancer, in that it maintains the momentum of the fuel jet (a factor critical to achieving high premixing quality), and as an ignition controller.

The design of the injector is crucial to the effectiveness of the carrier air in the above roles. The fuel lance was developed through a series of extensive tests as well as detailed computational analysis. 7 shows contours of the mean fuel concentration at the fuel nozzle exit, as obtained with a 3D computation of the turbulent flow and mixing within the fuel lance. The figure shows that the fuel is confined to the central part of the jet and is completely surrounded by the carrier air.

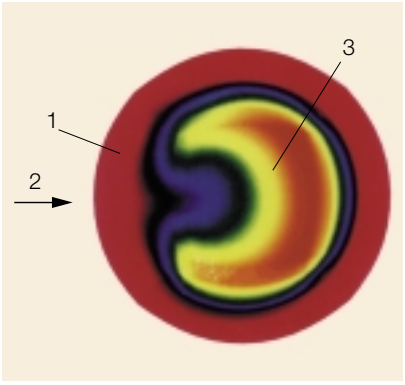

Calculated fuel mass fraction at injector outlet 7

1 *Carrier air*
2 *Main flow (HP turbine exit gas)*
3 *Fuel*

The delay in the ignition process resulting from the appearance of carrier air is illustrated in 8, which shows the ignition delay time as a function of fuel and carrier air concentrations for a typical SEV operation point. The figure shows results from idealized plug flow computations which are performed for each discrete initial mixture state using the CHEMKIN code [13]. The shortest ignition delay times are seen to occur at very lean mixtures, since the mixture temperature increases as the initial concentration of the hot exit gas of the HP turbine is increased.

As a fuel jet emerges into the hot exit gas of the HP turbine, short ignition delay times will be apparent over a wider range than exhibited in 8. As indicated above the ignition process is initiated in mixtures that occur at the extremities of the fuel jet. Although these regions are very lean and may result in a very low temperature rise, ignition will propagate very rapidly to other regions, as the heat and radicals are transported away from the ignition source to neighbouring regions through turbulent mixing. A key process in the control of both the ignition delay and emissions is therefore the turbulent mix-

Ignition delay time (based on maximum CH mole fraction) as a function of the initial composition for typical SEV operation 8

τ *Ignition delay*
f *Initial fuel mass fraction*

Red arrow *Increasing carrier air concentration*

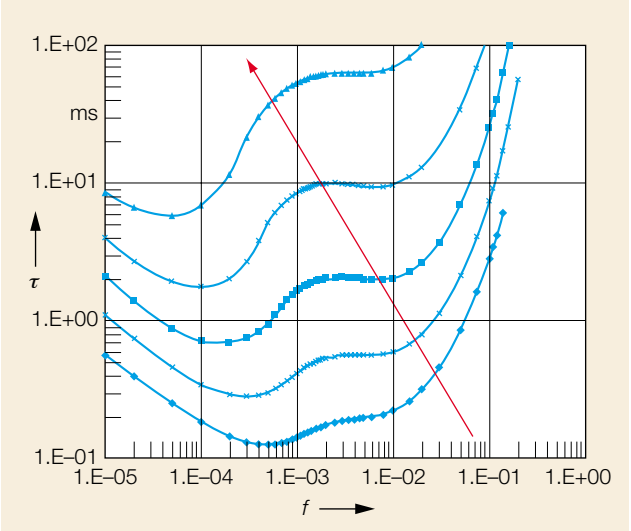

Fine scale mixing rate between fuel and HP turbine exit gas at plane 0.8 jet diameters from injector exit 9

1 *Injection hole*
2 *Main flow (HP turbine exit gas)*
3 *High mixing rates between HP turbine exit gas and fuel*

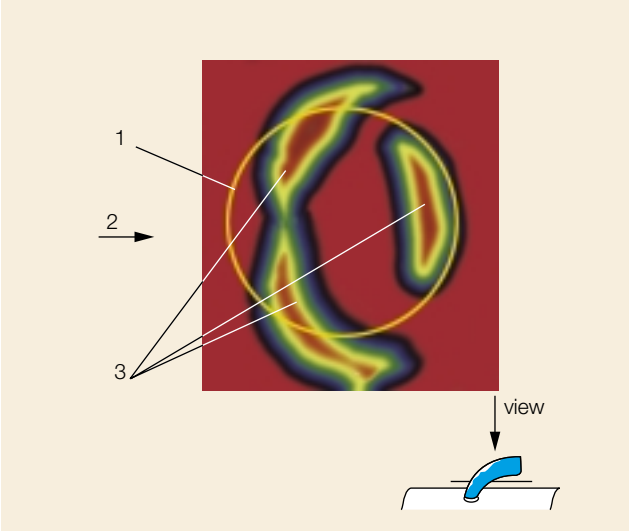

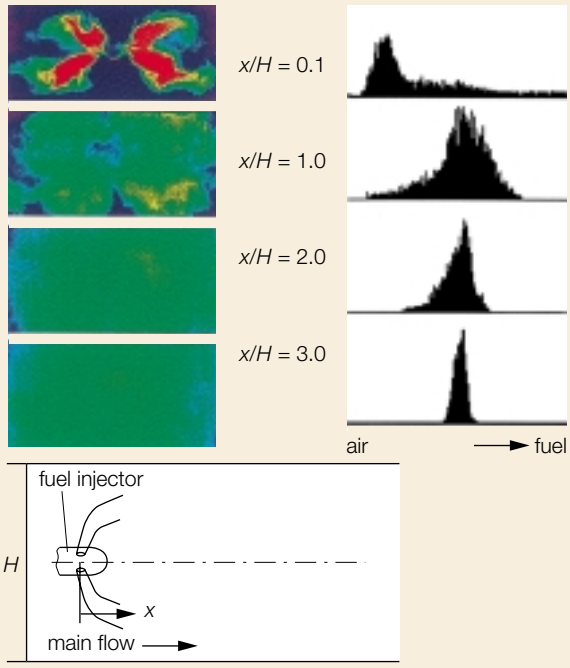

LIF pictures and associated histograms of transverse planes along the mixing section 10

x Axial coordinate
H Channel height

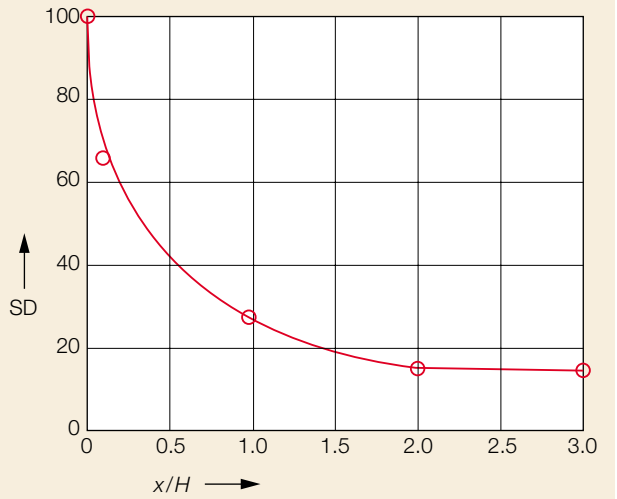

Variation coefficient (standard deviation/mean, SD) of the mixing quality versus the normalized axial distance x/H 11

x Axial coordinate
H Channel height

ing of the fuel, carrier air and HP turbine exit gas.

Fuel/air premixing

To better understand the coupling between the small-scale turbulent mixing and chemistry that controls ignition, the mixing of the fuel/carrier air jet and the HP turbine exit gas was studied by way of CFD. The commercial package CFDS-FLOW3D [2] was used for this, the turbulent flow being modelled by addressing density-weighted averaged variables. Turbulent closure was achieved using the two-equation k-ε turbulence model.

Given the non-linear dependence of the ignition chemistry on the state of the mixture, it is necessary to know the instantaneous state rather than just the mean mixture characteristics that are offered by the averaged balance equations. This issue has been effectively tackled within the modelling of turbulent non-premixed combustion, where the thermochemical field can be related to a single conserved scalar, eg the mixture fraction, by presuming the form of the probability density function (PDF) of the mixture fraction from its first two moments. The latter are obtained by solving the appropriate balance equations [4].

In the given circumstances, however, and considering that there are three separate streams – fuel, carrier air and HP turbine exit gas – the mixture field is described by two conserved scalars. Furthermore, the correlation between these streams is essential when inferring ignition delay behaviour. For a given instantaneous fuel concentration, the instantaneous rate of the ignition reactions are dependent upon the instantaneous carrier air concentration and the instantaneous hot gas concentration. Therefore, a two-dimensional joint PDF is necessary.

Within the confines of the SEV development programme, an approach based upon obtaining the joint PDF by solution of its transport equation [15] is not feasible due to the complex 3D flows and the need to rapidly assess the merits of different designs. Instead, the work described in [8] has been followed, whereby the joint PDF is presumed from a finite number of moments. The model is based on the assumption of a multi-variate beta-function PDF for the scalar variables. The PDF is then constructed from the first moments of each of its components and the turbulent scalar energy.

The above model has been used to investigate the turbulent mixing process and its coupling with the chemistry as well as to evaluate the attributes of differ-

ent lance designs in terms of the mixing and hence the ignition process. 9 shows the computed results of the modelled scalar dissipation rate based on the fuel and HP turbine exit gas, ie the rate at which fuel and hot gas mix at the molecular level, which is necessary for the chemical reaction to proceed. The fuel jet boundary condition used for the calculation is shown in 7. 9 indicates the region most vulnerable to self-ignition.

Aerodynamic and fuel/oxidant mixing within the burner

As in the EV burner, fuel distribution and mixing within the SEV burner is achieved with the aid of vortical flow. The flame is anchored at the vortex breakdown position. The vortices are generated by delta wings, formed like ramps and located on the walls of the SEV burner.

Water model tests were employed extensively throughout the development of the SEV combustor to lay out and optimize the burner aerodynamics. The preliminary tests were carried out in a straight channel, simulating first a single and later double annular segments of the SEV combustor. In this relatively simple test rig numerous concepts for the fuel injection, mixing and flame stabilization were investigated with regard to the mixing quality and velocity distribution along the mixing section. Another requirement was a single fuel supply per segment to facilitate reliable liquid fuel injection and ensure a simple and robust design. With all these restrictions in mind, a great number of variations of each alternative concept were set up and tested in a plexiglas test rig.

Laser Doppler anemometry was used to assess the mean and turbulent velocities along the mixing section and combustor. All three components of the velocity were measured. The primary aim of these measurements was to ensure that the axial velocity along the mixing section provides a large enough safety margin against flashback. Additionally, the swirl components of the velocity were measured in order to optimize the flame stabilization geometry 13.

Computed secondary flow patterns at the fuel injection plane (half channel width) 12

Vector plot of the radial and circumferential velocity components at the fuel injection plane as measured with LDA in a rectangular perspex model (half channel width) 13

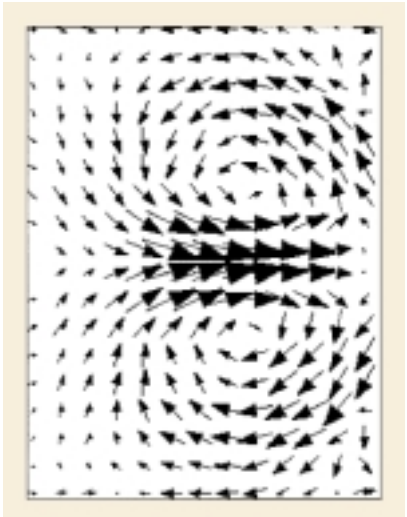

The fuel distribution and mixing quality were measured by means of Laser Induced Fluorescence (LIF). In this technique, the fuel flow is simulated by a solution of disodium fluorescence (a laser dye which fluoresces strongly when illuminated at the wavelength of 488 nm) in water. The main stream was seen to be free of dye. The blue line of an argon-ion laser is transmitted into the test section via a fiber optic cable and manipulated into a sheet by a cylindrical lens or rotating mirror. This light sheet illuminates a plane of 1 mm thickness, which is traversed along the mixing section to observe selected cross-sections via a CCD camera. Recordings made by this camera are digitized via a frame grabber and subsequently evaluated on a computer to obtain statistical values, such as mean and standard deviation. A series of grey scale pictures for a specific injector and mixer configuration are given in 10 for consecutive transverse planes downstream of the injection point.

Next to each picture is a histogram showing the distribution of the pixels with a certain grey scale value. These histograms focus on just the lean region of the fuel jet. A peak at the left end of the diagram means pure air. At $x/H = 0.1$ the peak is associated with water free of dye, whilst at $x/H = 3.0$ it is centered around the perfect mixture. It can be seen from these histograms that the mixing progresses rapidly to yield a very narrow distribution. The progress of the standard deviation of the mean ratio (defined as a variation coefficient) is shown in 11.

CFD calculations were performed alongside the combustion and water tests during development of the combustor in order to obtain a robust design in

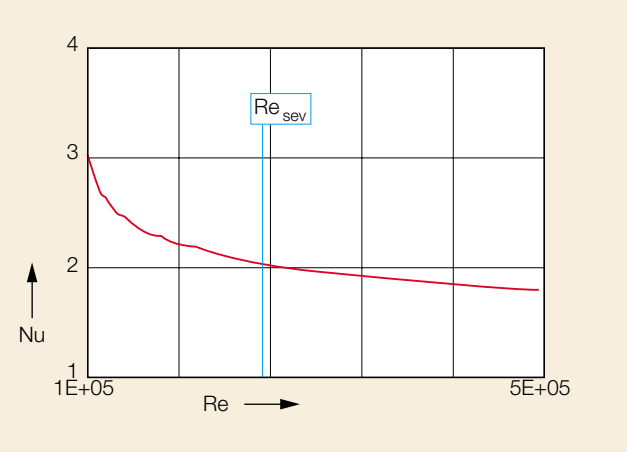

Nu enhancement behind a backward facing step **14**

Nu *Nusselt number*
Re *Reynolds number*

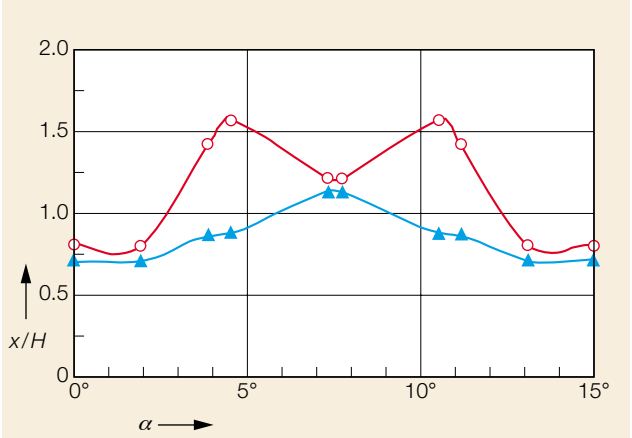

Non-dimensional reattachment length behind the SEV backward facing step from CFD simulation **15**

x/H *Reattachment length*
α *Circumferential angle from one wall to other wall of SEV burner*

Outer SEV liner
Inner SEV liner

the shortest possible time at minimum cost. With regard to the aerodynamic design of the SEV burner, CFD was used for:

- Preliminary and rapid analysis of initial designs and subsequent modifications, and of the influence of all the boundary conditions under which the combustor operates.
- A better analysis of the test data through the detailed study of the processes.

Given the vortical turbulent flows that occur within the SEV combustor, it is essential for the CFD to be strongly coupled to the testing activities in order to be able to gauge the reliability of the CFD results and assess the extent to which CFD should be relied upon. Comparison of water test results and CFD results have shown that the accuracy of the aerodynamics data is sufficient to allow CFD to be used for assessing the geometry and boundary condition modifications.

12 shows the computed secondary flow pattern downstream of the vortex generators within the SEV burner. The computations were performed using CFDS-FLOW3D and the standard k-ε turbulence model to achieve closure of the mean balance equations. Although the standard k-ε model is not well suited to swirling flows, the adopted strategy results in a good balance between accurate results and an acceptable turnaround time for the computations.

A comparison of the computed and the measured secondary flow field **12**, **13** shows that the major flow features are reproduced.

SEV combustor cooling technology

An innovative cooling system was developed which meets all the requirements of the self-igniting premixed SEV combustion chamber. Minimization of the combustor's cooling air consumption was an important goal during development of the sequential combustion system because the cooling air of the SEV combustor bypasses the HP turbine. Such requirements are in contrast to those for a convective cooled combustor in a standard cycle gas turbine, where the pressure drop must be minimized and therefore the maximum amount of air must be used for cooling. Special attention was also paid to ensuring that the hardware is of a robust construction and that variations in the boundary conditions would have only a minimal influence on the effectiveness of the cooling.

Essentially, a counterflow cooling system with full heat recuperation is used, in which virtually all the cooling air is mixed with the hot gas from the HP turbine ahead of the flame. After having cooled the combustor liner walls via convective cooling, the cooling air is injected into the hot gas path via the effusion cooling of the burner. The full amount of cooling air is used to reduce the flame zone temperatures, and therefore the NO_x emissions.

Due to the high Re number flow and the premix character of the flame, the dominant heat transfer mechanism within the SEV combustor is convection. Only 1/5 of the total heat flux rate is attributed

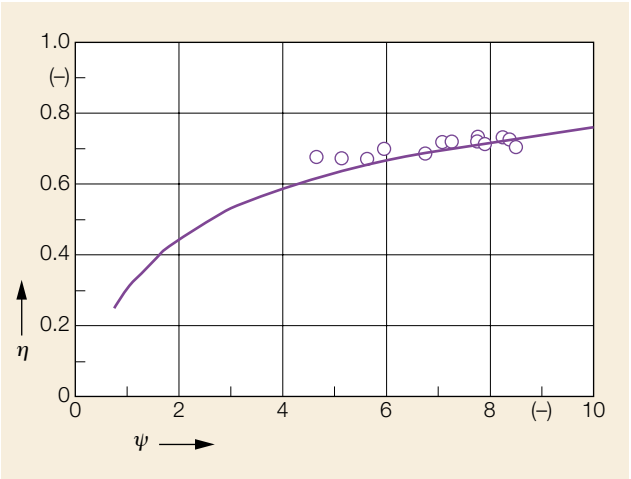

Cooling effectiveness of the SEV liner, measured during the high-pressure test 16

η Cooling effectiveness
ψ Coolant mass flow function

○ Measurements
– Ideal trend

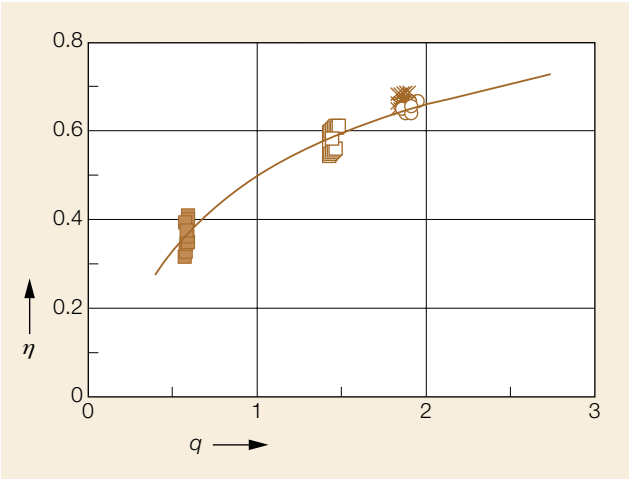

Axial development of the effectiveness of effusion cooling of the SEV burner, measured during the high-pressure test 17

η Cooling effectiveness
q Local heat load parameter

■ Vortex generators
□ Fuel injection
× Mixing zone
○ Backward facing step
– Ideal trend

to the radiation of the non-luminous flame.

The peak wall heat transfer within the SEV combustor is dominated by the convection of the reacting flow resulting from the sudden expansion at the exit of the SEV burner. The turbulent shear layer starting at the apex of the backward facing step reattaches to the liner wall several step heights downstream, where it causes a local peak in the heat transfer. For a given expansion ratio the peak Nusselt number of an unswirled flow scales with $Re^{2/3}$, while in a fully developed flow Nu grows like $Re^{0.8}$. Scaling up the available data [20, 3] to higher Re leads to an Nu enhancement factor of 2 behind the backward facing step 14.

Detailed CFD simulations 15 showed the average reattachment length of the swirled SEV burner flow to be only 1.2 times the premixing channel height, which is only 2/3 the value for a tubular single swirler flow [6]. This earlier reattachment is attributed both to the multi-swirler flow within the SEV burner and the annular geometry of the combustion chamber.

The hot gas heat transfer modelling was then based on the stated Nu value, assuming a typical boundary layer development downstream of the calculated location of the flow reattachment, and includes the flame radiation.

In recent years ABB has amassed a considerable amount of experience in the use of thermal barrier coatings (TBC) on tiles in combustor cooling systems. The protective layer, which reduces thermal loading at its source (on the hot-gas side) is built up by spraying on a coating of zirconia oxide (ZrO2). The benefits of the TBC were mainly used to lower the liner wall temperature to levels where superior metal properties allow a significantly longer lifetime for the components than before.

All the SEV cooling air enters the liner cooling system near the LP turbine, thereby locally cooling the contraction ahead of the turbine via an impingement plate. Afterwards, the air travels upstream.

The cross-sectional area of the cooling channel is gradually reduced to counterbalance the effect of the heat picked up by the cooling air and to adjust the effectiveness of the local cooling to the varying heat input from the hot gas. In addition, the heat transfer is enhanced by turbulators at the cooling channel wall [10,11].

16 shows the measured effectiveness (ie, the dimensionless wall-metal temperature on the hot-gas side) of the liner cooling as a function of the coolant mass flow function. The latter is defined as the ratio of the heat capacity rate of the cooling air to that of the hot gas wetted surface, and therefore as the inverse of the number of heat transfer units used in heat-exchanger theory [12]. In high-

pressure tests under real machine conditions all the combustor liner temperatures remained well below 800 °C, thus providing empirical support for the modelling of the heat transfer process.

After having cooled both liners of the combustion chamber the air is discharged into a plenum chamber surrounding the SEV burners. This cavity damps out all possible flow non-uniformities ahead of the burner cooling so that a common pre-pressure drives the effusion cooling.

Effusion cooling, sometimes referred as full coverage film cooling [12], is a relatively recent development in combustor cooling technology and has not been used widely until now. A large number of small, straight holes drilled in the single-sheet wall to be cooled are arranged in such a way that three basic heat transfer mechanisms interact to ensure highly effective cooling:

- Coolant film on the hot-gas side
- Internal convection inside the effusion holes
- Heat transfer on the back wall where the coolant enters the holes

An effusion cooling model has been proposed [9] together with the key parameters for correlating measured data from effusion heat transfer experiments with respect to the different heat transfer effects.

Before the burner cooling design was laid out this model was used to define a basic test series under atmospheric conditions; the cooling efficiency of different effusion test plates was measured, with subsequent variation in the parameters affecting the different cooling mechanisms. The influence of the longitudinal vortices within the burner on the development of the film cooling was also investigated in detail. All the measured data were correlated with respect to the three different factors contributing to heat transfer, as stated above, in order to derive a physically based layout guideline for effusion cooling.

The local effusion hole spacing was chosen to give an optimum balance between the internal heat transfer rate and the film cooling effect, thus reducing the temperature gradient across the burner. The effusion jet to hot-gas momentum ratio was kept below unity; the result is a well-defined film development, while the cooling jets are prevented from being lifted off into the hot-gas stream. Because of the large area through which the cooling air is effused and the good mixing properties of the helical swirling motion within the burner, mixing ahead of the flame is highly uniform. An additional feature of this effusion cooling is the cold and fuel-lean wall boundary layer, which inherently prevents the flame from travel-

SEV combustor test rig **18**

1 *Gas inlet*
2 *Pressure vessel*
3 *Gas exit*
4 *Combustor*
5 *Burner*
6 *Fuel injector*
7 *Two-burner sector*

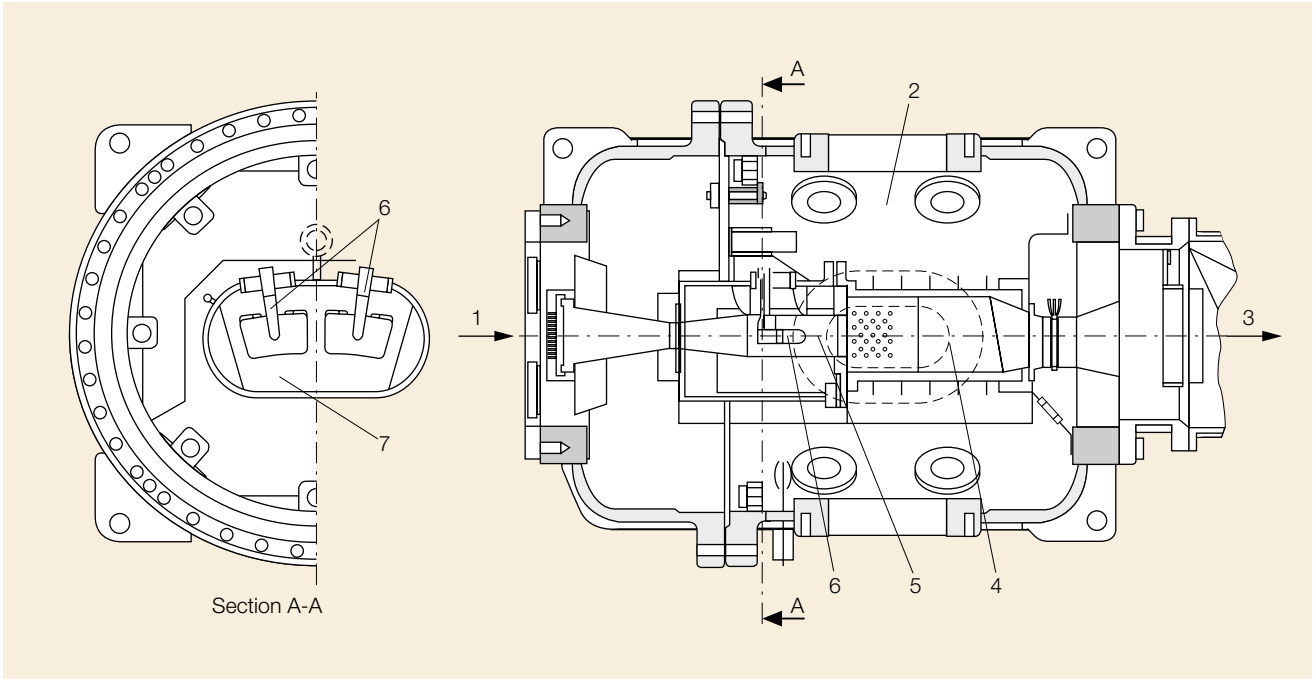

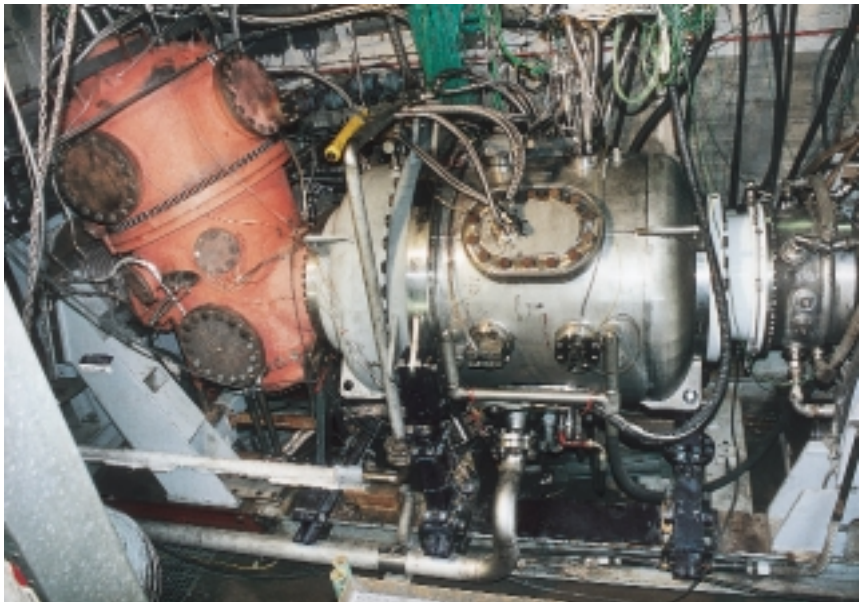

SEV combustor test rig with hot gas supplier (left) and SEV pressure vessel (right) 19

ling upstream via the low velocity region near the wall.

The effectiveness of the effusion cooling within the SEV burner is shown in 17 with respect to the axial position as measured in the high-pressure test with real machine parts. The heat load parameter is defined as the local coolant to hot gas ratio of the heat transfer coefficient times the wetted area. The related burner wall temperatures all remained well below 850 °C.

The combined result of this and the convective liner cooling is a highly effective and very robust cooling system with a cooling air consumption minimized to only 1/10 of the combustor exit flow rate.

Validation of the SEV combustion chamber design

Tests were carried out in steps during the development of the SEV combustor. Conceptual tests and primary feasibility studies were performed under atmospheric pressure conditions to demonstrate the feasibility of self-ignition. Subsequent tests investigated the qualitative influence of various parameters, such as inlet conditions and different configurations for the injectors and turbulence generators.

The next step was to test at elevated pressure to demonstrate the basic principle of premixing and self-ignition under machine conditions. NO_x formation and CO burn-out were also investigated during these tests. The SEV combustor test rig consists of two independent combustors in a serial arrangement. The first combustor acts as a hot gas generator and simulates the SEV combustor inlet conditions, while the second combustor is the SEV arrangement to be tested.

The final design of the combustor was validated using a two-sector, original-sized test rig under real machine conditions. Parts such as the burners, fuel lances and liner segments were identical with the real machine parts.

18 shows the high-pressure test rig with the two-sector model of the SEV combustor inside a pressure vessel. The real inlet conditions were simulated by an EV combustor feeding hot gas into the SEV combustor. This arrangement allowed the air pressure at the combustor inlet, the air temperatures and the mass flows to be adjusted correctly.

The measuring equipment consists of thermocouples at several stations between the burner lance and the liner segments. Exhaust emissions could be measured at three axial positions using water-cooled integral probes, each with 5 holes located radially. The pressure drop across the sampling holes was such that quenching was ensured under all conditions. Five probes were positioned at different circumferential locations at the combustor exit. The mixing section of the burner, from the fuel injection point to the combustor, could be observed by means of a video system.

19 shows a view of the test rig with the two combustors on the high-pressure test facility. The tests were carried out for conditions ranging from SEV ignition to full load. Stable combustion inside the combustor could be observed throughout the operating range.

The NO_x formed in the SEV combustor is shown in 20 in relation to the simulated machine load. The units used are g_{NOx}/kg_{fuel}, which gives the emission values without the influence of the O_2-content of the exhaust gas. No NO_x formation was measured in the SEV combustor under low-load conditions. NO_x formation increases up to about 1 g/kg_{fuel} at 100 % load.

To obtain the NO_x emissions of the machine by extrapolating the NO_x produced by the SEV combustor, it is necessary to consider the fuel mass flow rates of both combustors. 21 shows the expected engine NO_x emissions of the machine under typical full-load conditions for assumed EV combustor emissions of 18 and 12 vppm NO_x. With no NO_x produced in the

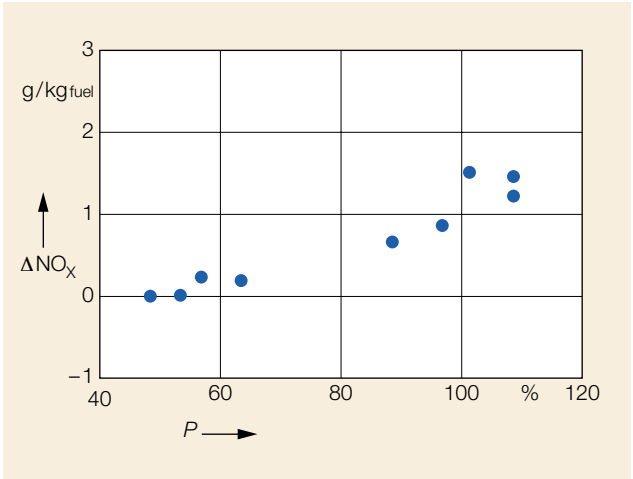

Measured NO_x formation in the SEV combustor in relation to the simulated machine load P (two-sector rig) 20

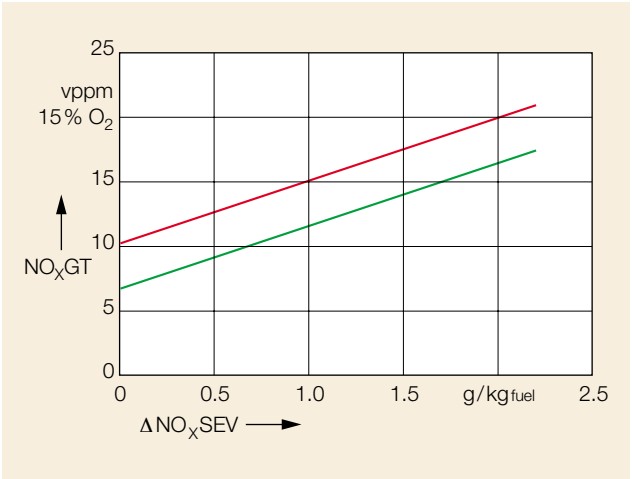

NO_x emissions of machine as a function of the NO_x emissions of the SEV and EV combustors 21

NO_xGT *Gas turbine NO_x emissions*
ΔNO_xSEV *NO_x production of SEV combustor*

Red *18 vppm NO_x assumed emitted by EV combustor*
Green *12 vppm NO_x assumed emitted by EV combustor*

SEV combustor, the NO_x emissions of the EV combustor would be reduced from 18 vppm to 11 vppm. For an SEV NO_x formation of 1 g_{NOx}/kg_{fuel} the NO_x emissions of the machine are expected to be 15 vppm (15 % O_2), based on the EV NO_x amount of 18 vppm.

These investigations clearly indicate that there is a potential for reducing the emissions to levels in the single digit range.

The volume of the combustor has been sized for good CO burn-out down to low-load conditions using emission measurements under real machine conditions at several axial distances in an initial test combustor. 22 shows the results of the subsequent two-sector validation test results. The measured UHC emissions are very low, as 23 shows.

Measured carbon monoxide emissions (CO) under simulated machine load (P) conditions (two-sector rig) 22

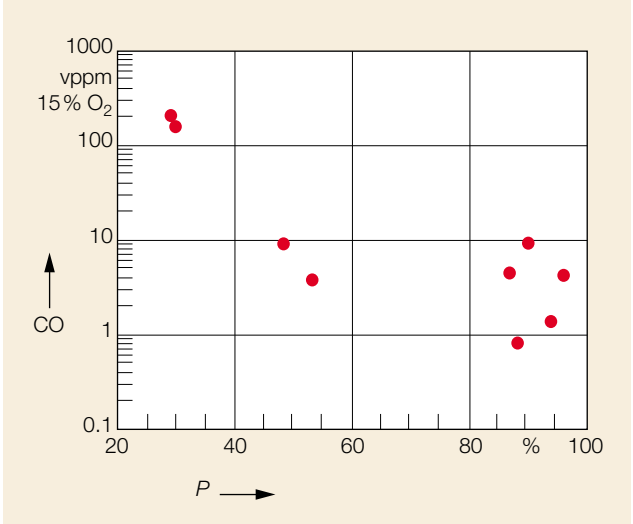

Measured unburned hydrocarbon emissions (UHC) under simulated machine load (P) conditions (C_3H_8, two-sector rig) 23

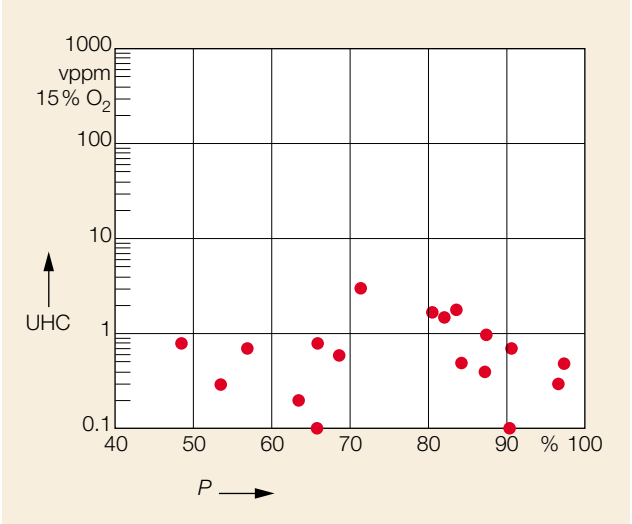

Summary

Sequential combustion was chosen for the GT24/GT26 gas turbines in order to achieve high cycle efficiency at moderate turbine inlet temperatures as well as optimum gas turbine exhaust temperatures for the steam cycle in combined cycle applications. The design of the first combustor, the EV combustor, is proven in more than 800,000 operating hours. The reliability of the second combustor, the SEV combustor, has been validated by several fundamental investigations as well as tests using machine parts under real machine conditions. These tests demonstrated safe operation as well as low NOx, CO and UHC emissions for this design.

References

[1] M. Aigner, A. Mayer, P. Schiessel, W. Strittmatter: Second generation low emission combustors for ABB gas turbines: tests under full engine conditions. ASME 90-GT- 308, 1990.

[2] CFDS-FLOW3D, release 3.3: User manual. AEA Technology, 1994, Harwell, England.

[3] J. Baughn, M. Hoffmann, R. Takahashi, B. Launder: Local heat transfer downstream of an abrupt expansion in a circular channel with constant wall heat flux. Journal of Heat Transfer, 1984, vol 106, 789–796.

[4] R. W. Bilger: Turbulent jet diffusion flames. Progress in energy and combustion science, 1976, vol 1, 87–109.

[5] H. F. Coward, G. W. Jones: Limits of flammability of gases and vapors. US Bureau of Mines, Washington, 1976, bulletin 503.

[6] P. Dellenback, J. Sanger, D. Metzger: Heat transfer in coaxial jet mixing with swirled inner jet. Journal of Heat Transfer, 1994, vol 116, 864–870.

[7] H. U. Frutschi: Advanced cycle system with new GT24/GT26 turbines – historical background. ABB Review 1/94, 21–25.

[8] S. S. Girimaji: Assumed beta-pdf model for turbulent mixing: validation and extension to multiple scalar mixing. Comb Sci Tech, 1991, vol 78, 177–196.

[9] W. Hahn, G. Urner: Untersuchungen zu effusions-gekühlten Brennkammerelementen. Brennstoff-Wärme-Kraft, 1994, vol 46, no 12, 33–39.

[10] J. Han: Heat transfer and friction characteristics in rectangular channels with rib turbulators. ASME Journal of Heat Transfer, 1988, vol 110, 321–328.

[11] J. Han, J. Park: Developing heat transfer in rectangular channels with rib turbulators. Int Journal of Heat and Mass Transfer, 1988, vol 31, no 1, 183–195.

[12] W. M. Kays, M. E. Crawford: Convective heat and mass transfer. McGraw-Hill, New York, 1993.

[13] R. J. Kee, F. M. Rupley, J. A. Miller: CHEMKIN-II: A Fortran chemical kinetics package for the analysis of gas phase chemical kinetics. Sandia Report SAND89-8009B UC-706, 1989.

[14] T. Meindl, F. Farkas, R. Klussmann: The development of a multistage compressor for heavy duty industrial gas turbines. ASME Houston, 95-GT-371, 1995.

[15] S .B. Pope: PDF methods for turbulent reactive flows. Progress in Energy and Combustion Science, 1985, vol 11, 119–192.

[16] T. Sattelmayer, M. Felchlin, J. Haumann, J. Hellat, D. Steyner: Second generation low emission combustors for ABB gas turbines: burner development and tests at atmospheric pressure. ASME 90-GT-162, 1990.

[17] P. Senior, E. Lutum, W. Polifke, T. Sattelmayer: Combustion technology of the ABB GT13E2 annular combustor. 20th CIMAC G22 1993 London.

[18] L. J. Spadaccini, J. A. TeVelde: Autoignition characteristics of aircraft type fuels. Combustion and Flame 46: 283–300, 1982.

[19] L. J. Spadaccini, M. B. Colket: Ignition delay characteristics of methane fuels. Prog Energ Comb Sci, 1994, vol 20, 431–460.

[20] P. Zemanick, R. Dougall: Local heat transfer downstream of abrupt circular channel experiment. ASME Journal of Heat Transfer, 1970, vol 92, 53–60.

Authors

Dr. Franz Joos
Philipp Brunner
Dr. Burkhard Schulte-Werning
Dr. Khawar Syed
ABB Power Generation Ltd
P.O. box
CH-5401 Baden
Switzerland
Telefax: +41 56 205 8254
E-mail:
franz.joos@chkra.mail.abb.com
philipp.brunner@chkra.mail.abb.com

Dr. Adnan Eroglu
ABB Corporate Research
Segelhof
CH-5405 Baden-Dättwil
Switzerland
Telefax: +41 56 486 7359
E-mail:
adnan.eroglu@chcrc.mail.abb.com